Supplement of Atmos. Chem. Phys., 25, 12379–12407, 2025
https://doi.org/10.5194/acp-25-12379-2025-supplement

Atmospheric Chemistry and Physics Open Access

Supplement of

Global atmospheric inversion of the anthropogenic NH_3 emissions over 2019–2022 using the LMDZ-INCA chemistry transport model and the IASI NH_3 observations

Pramod Kumar et al.

Correspondence to: Pramod Kumar (pramod.kumar@lsce.ipsl.fr)

List of Figures

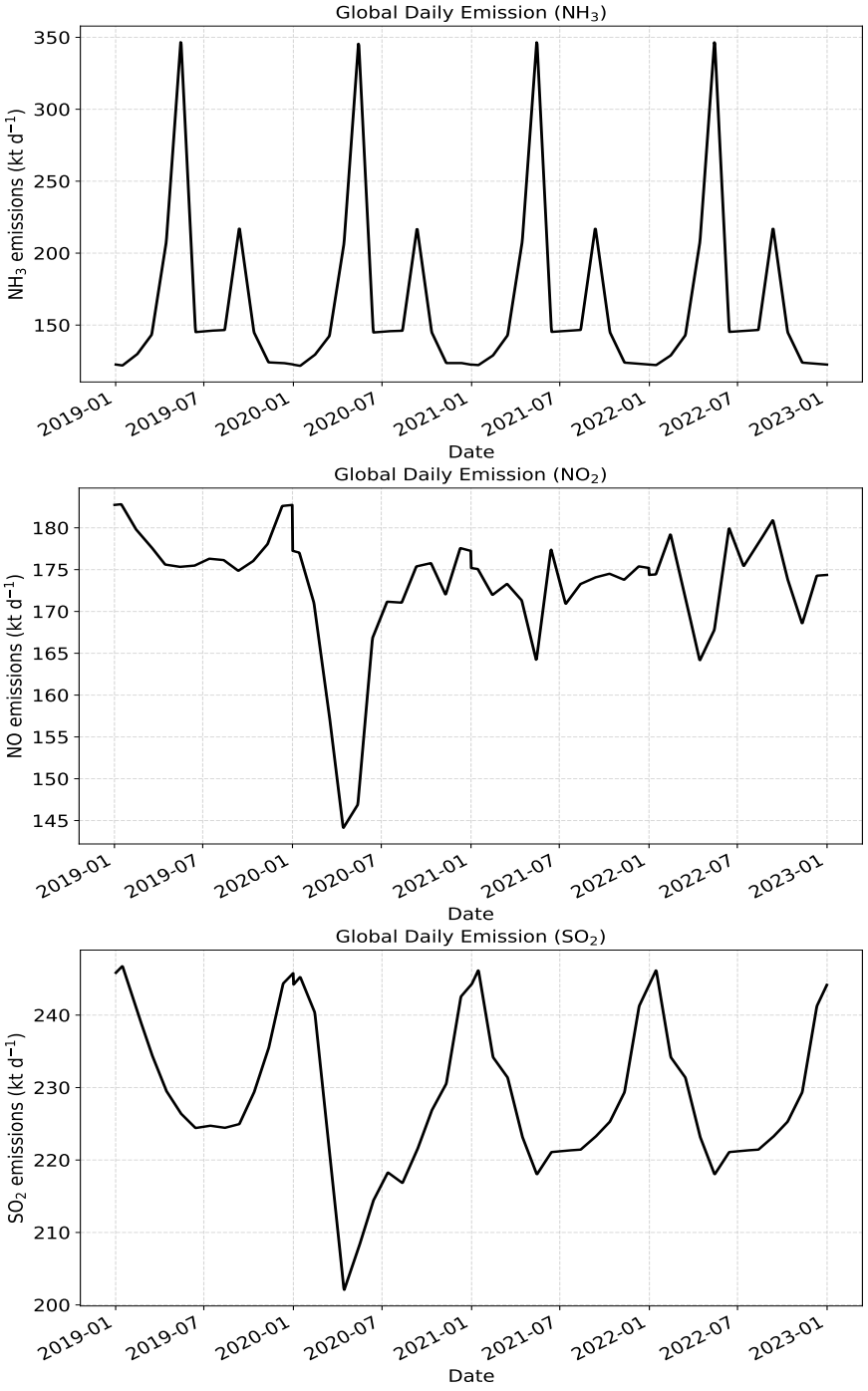

Figure S1. Global daily emissions (2019-2022) of (a) NH3, (b) NOx (as NO), and (c) SO2 from the prior CEDS anthropogenic and natural sources over the land.

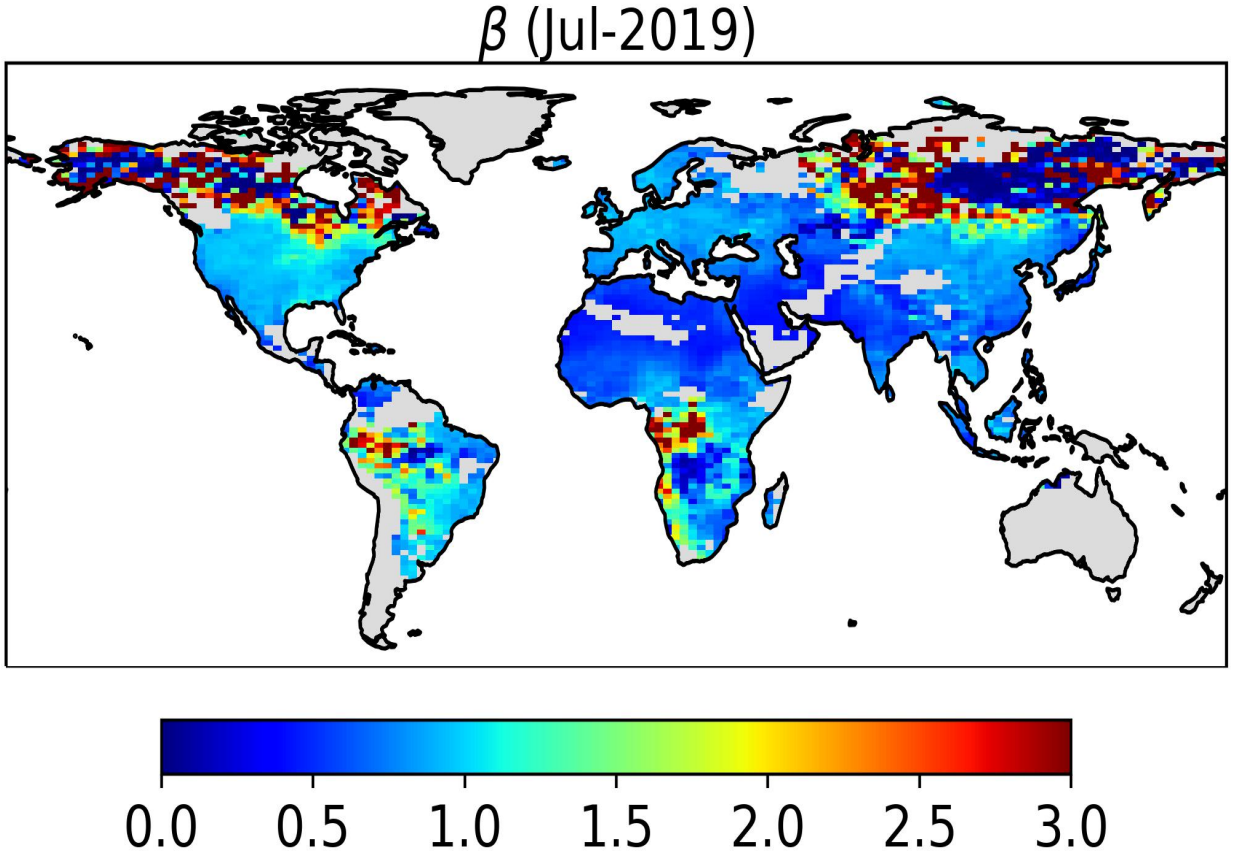

Figure S2. Spatial distribution of monthly mean β for July 2019.

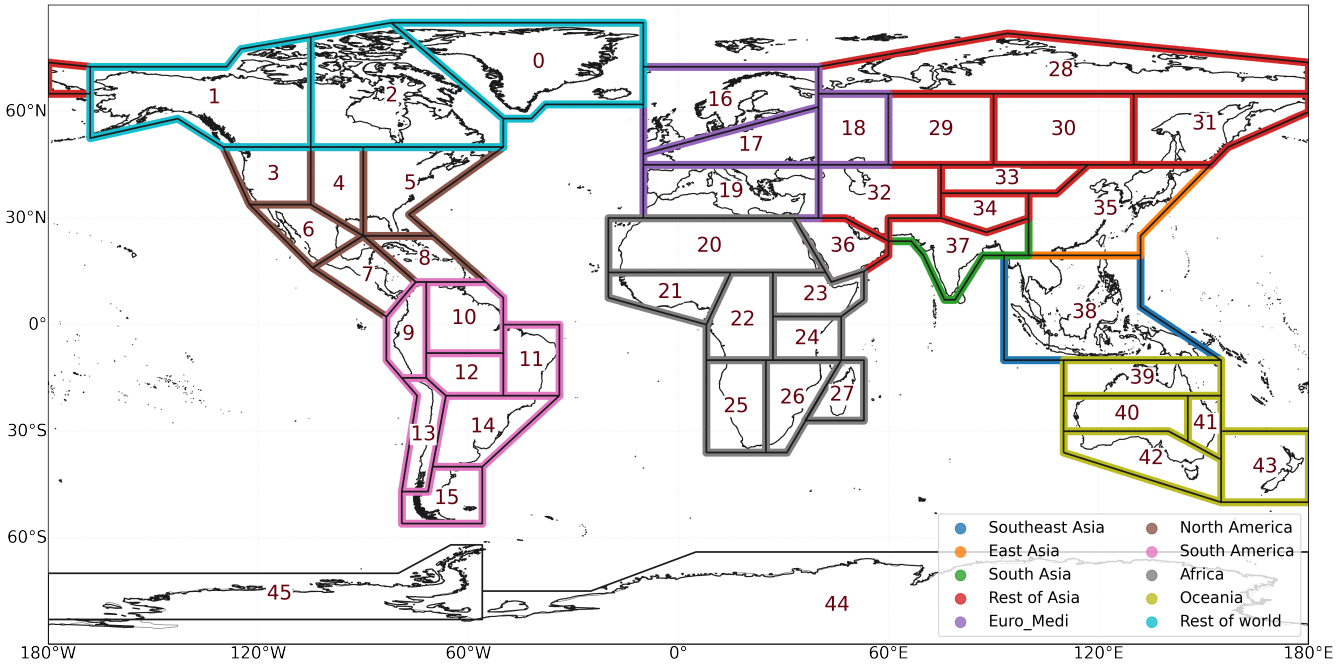

Figure S3. The boundaries of the 10 regions over the main land defined by **?** (based on the IPCC reference regions described in **?** used to gap filling the unconstrained emissions in this study.

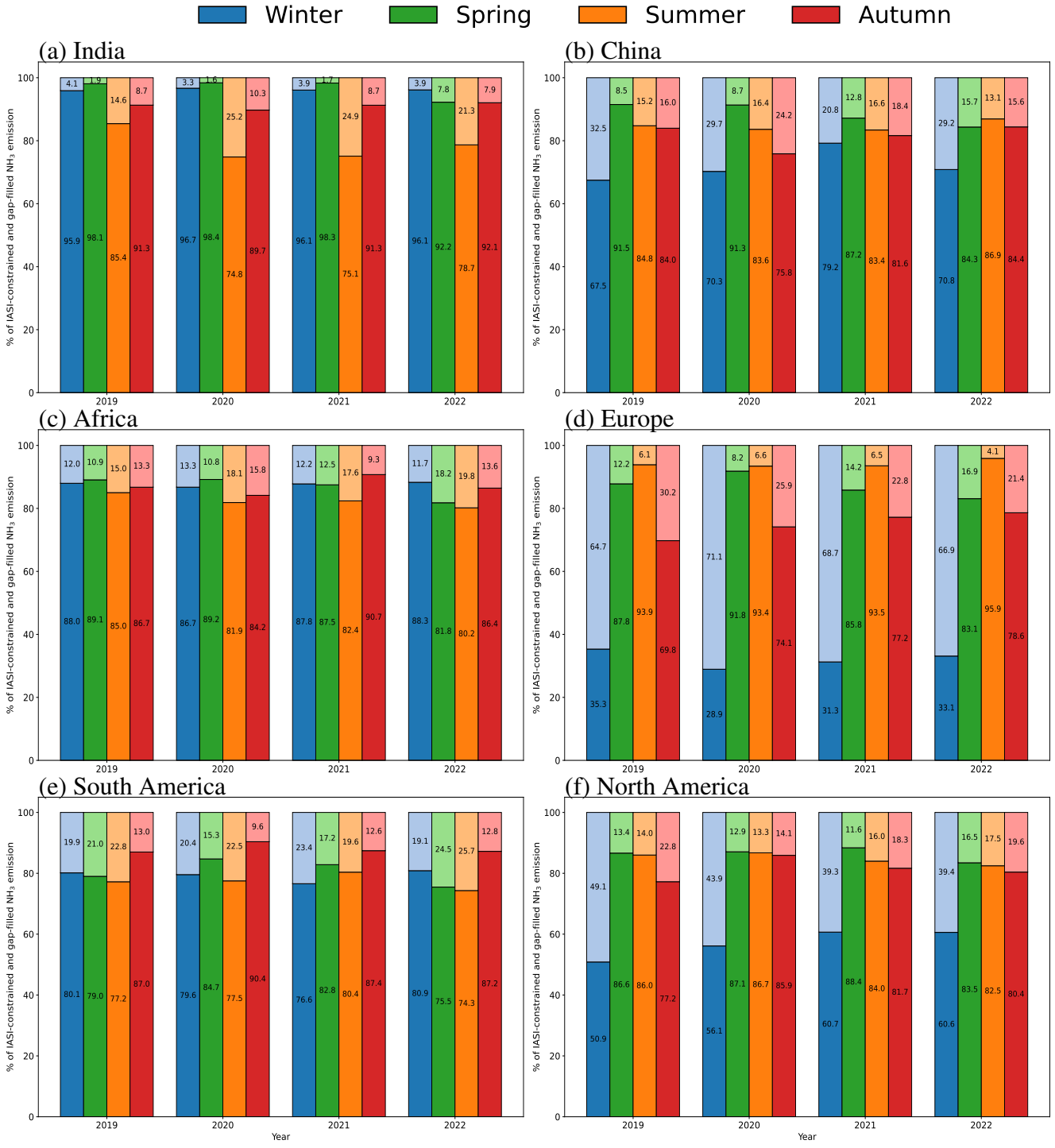

Figure S4. IASI-constrained (lower stack bars) and gap-filled (upper stack bars) percentage (%) of seasonal total NH_3 emissions across six regions over the land from 2019 to 2022.

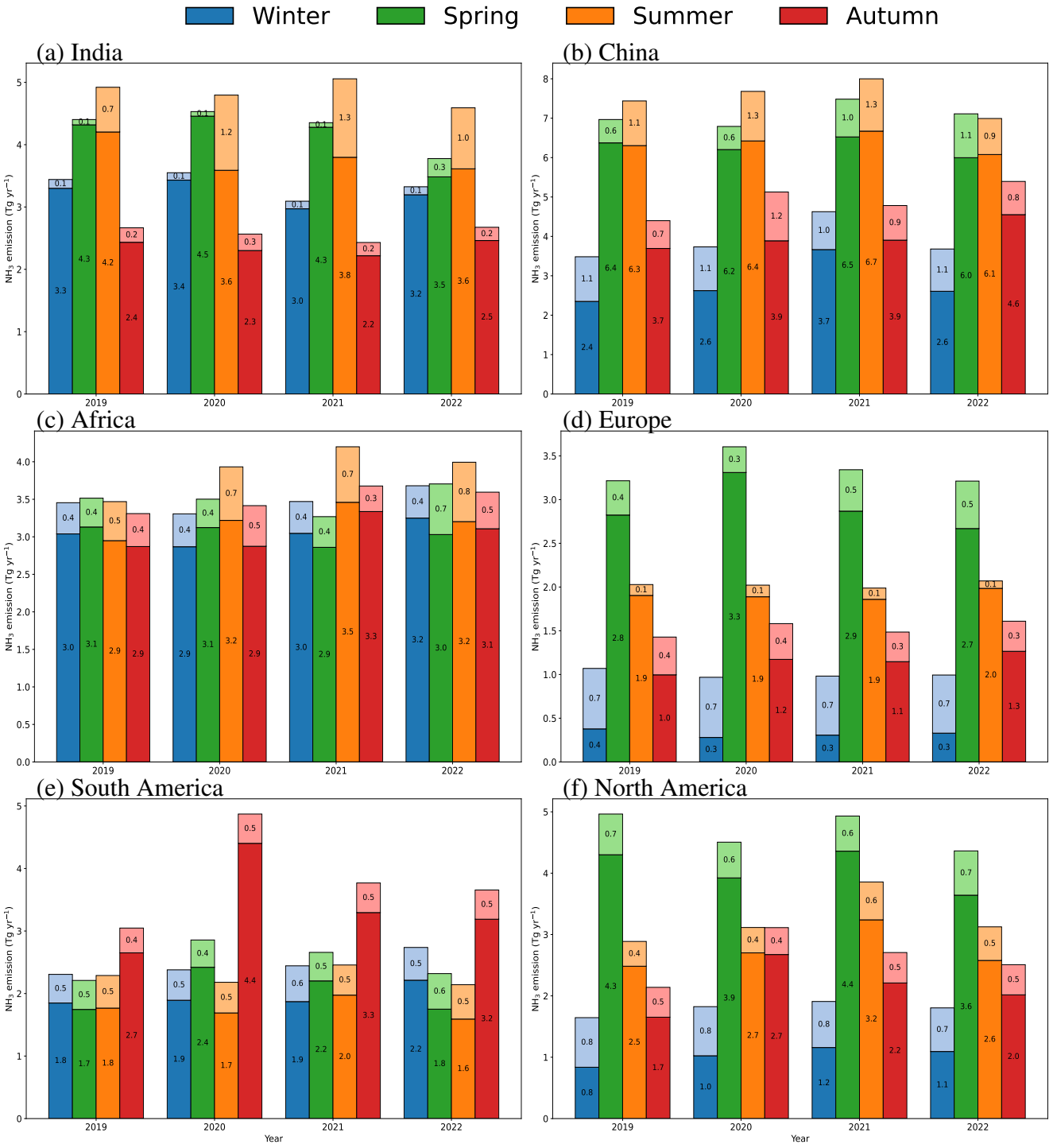

Figure S5. Seasonal NH_3 emissions (IASI-constrained (lower stack bars) and gap-filled (upper stack bars)) across six regions over the land from 2019 to 2022.

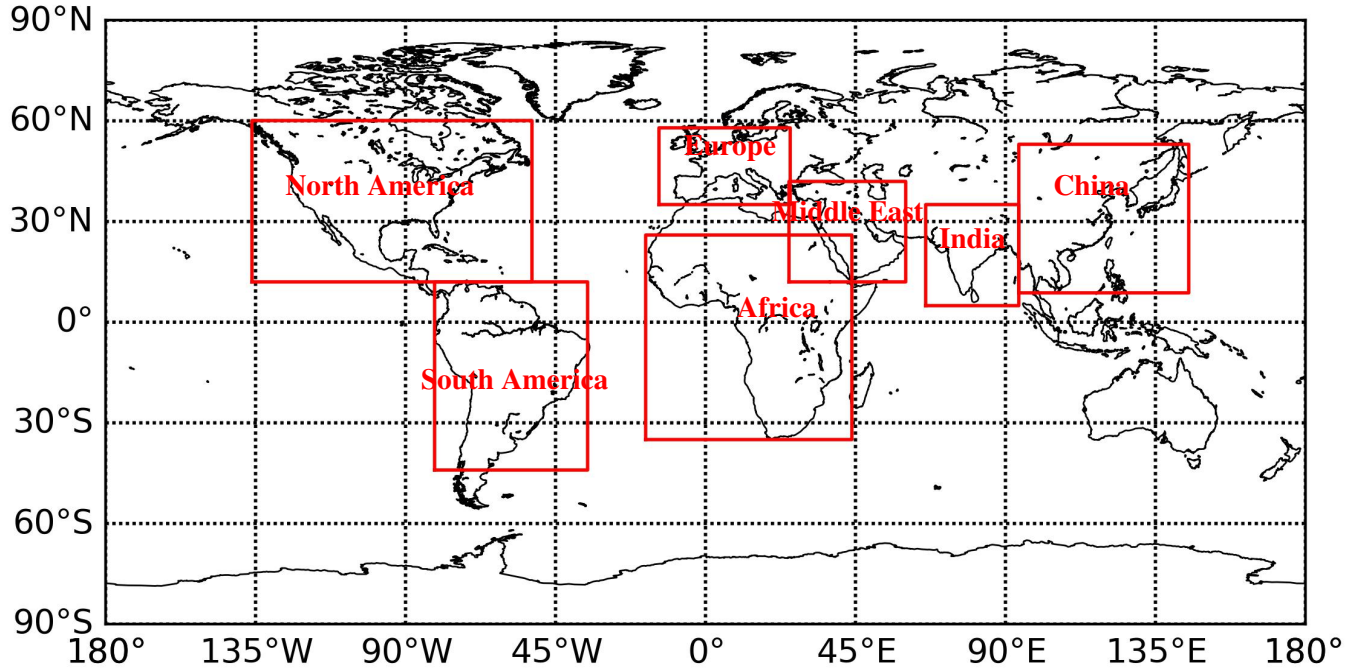

Figure S6. The regions selected for the regional analysis.

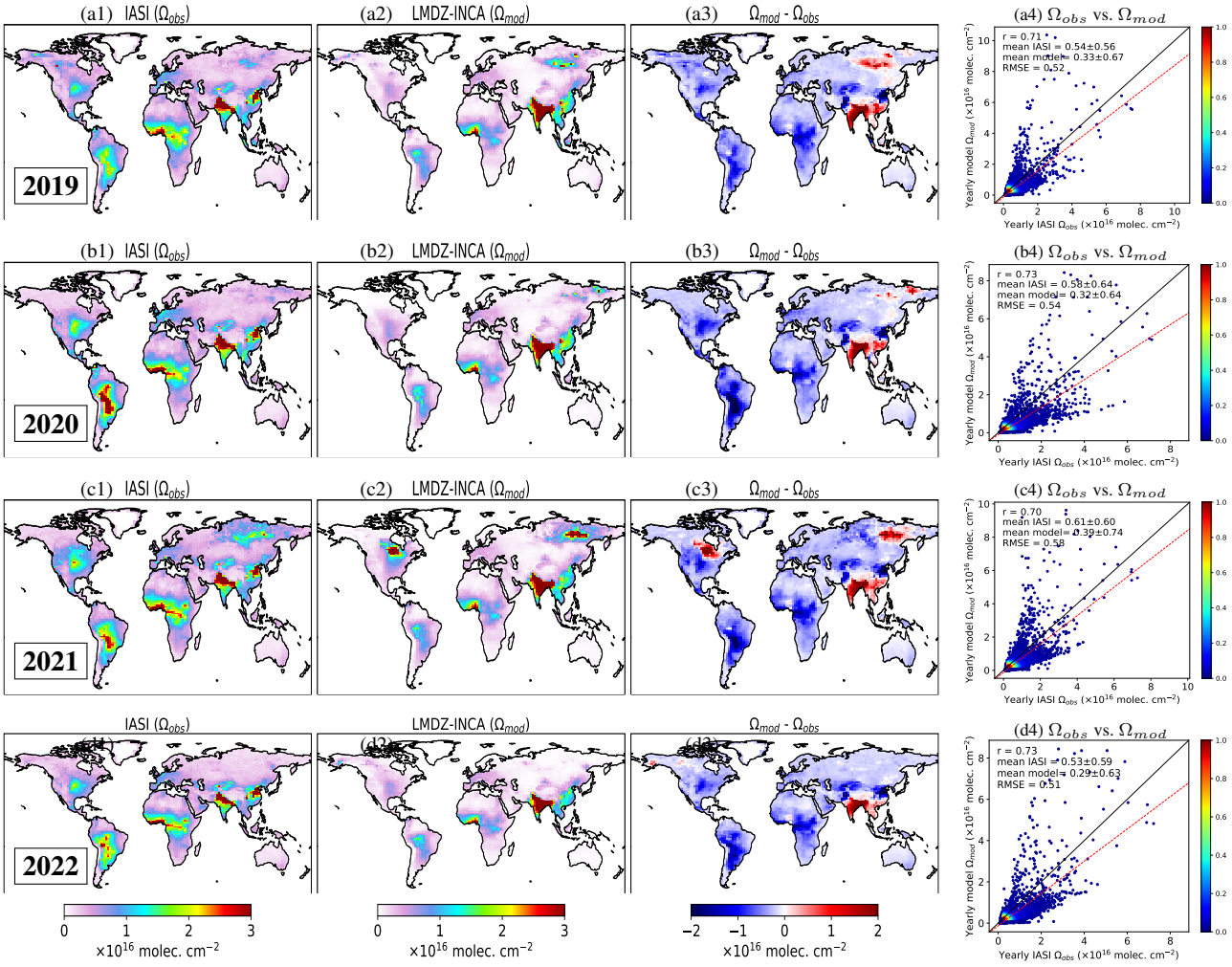

Figure S7. The spatial distributions of the annual mean NH_3 total columns for all four years from 2019 to 2022. The first and second columns in each row show annual mean from IASI ANNI-NH3-v4 observations (Ω_{obs}) and LMDZ-INCA model simulated columns after applying the averaging kernel (Ω_{mod}), respectively. The third column's figures show the differences Ω_{mod}- Ω_{obs} between. The last column figures show the scatter density plots between the observed IASI and the LMDZ-INCA model NH_3 columns. In the scatter plots, the solid blue line represents the one-to-one line, while the dashed red line represents the regression line.

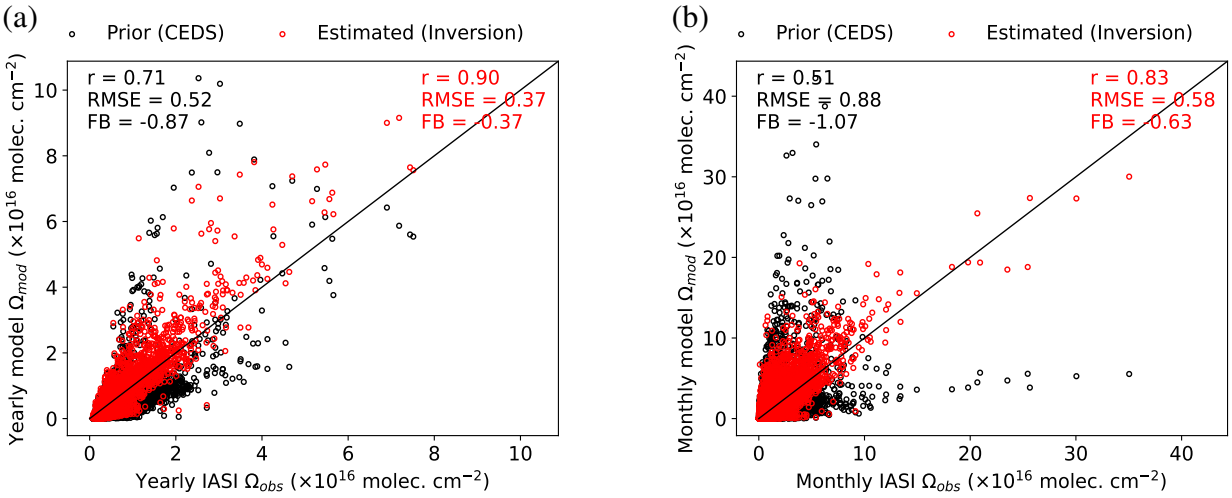

Figure S8. Comparison of the (a) annually, and (b) monthly averages of the IASI NH3 column observations (Ω_{obs}) over the model horizontal land grid cells at $1.27° \times 2.5°$ resolution to the corresponding simulations of average columns with LMDZ-INCA (Ω_{mod}) using the IASI-constrained NH3 emission estimates derived from our global inversions and using the prior CEDS NH3 emissions over the globe and the year 2019. It also shows the correlation coefficient (r) and root mean square error (RMSE), and Fractional Bias (FB) from this comparison. The black line denotes the one-to-one line.

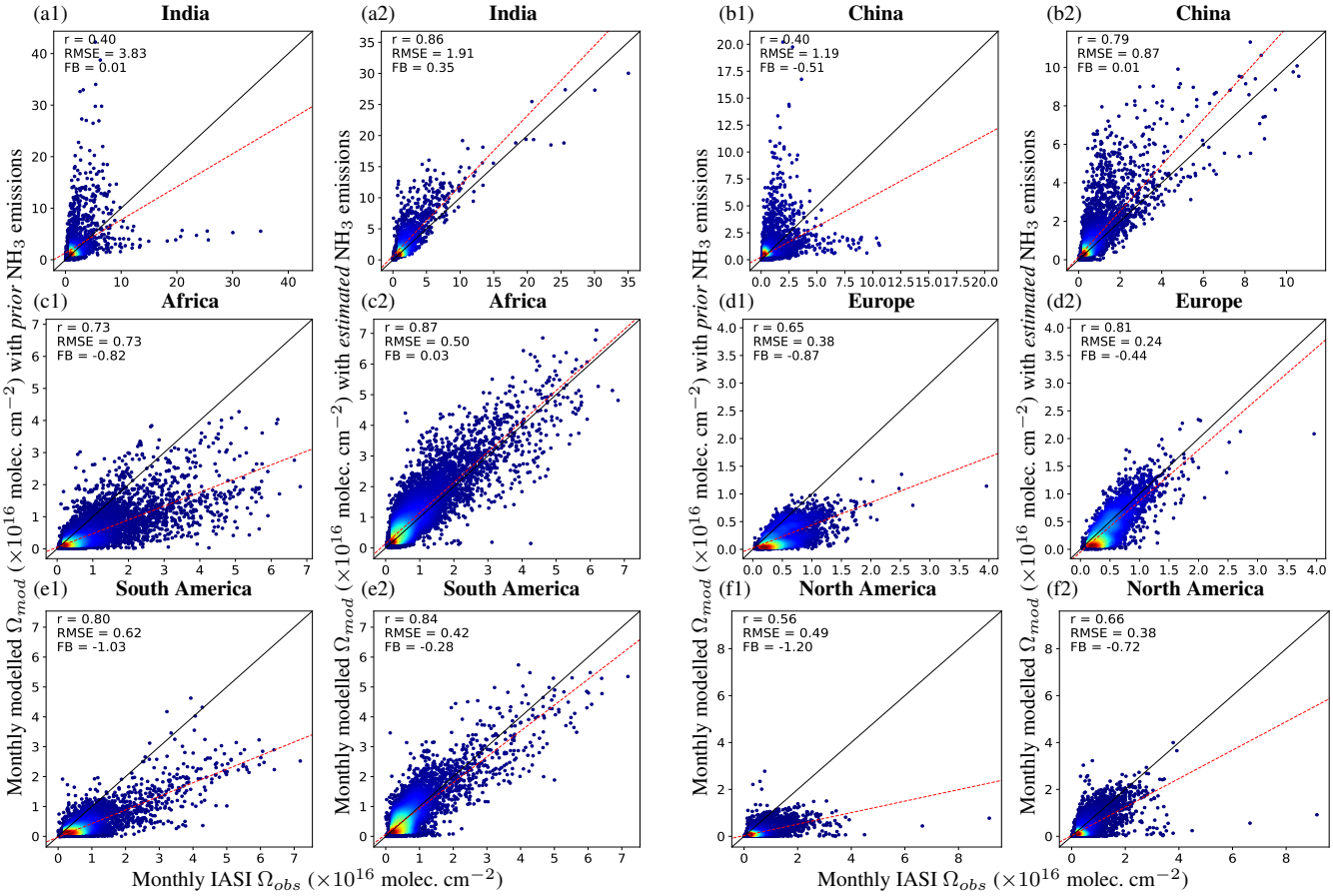

Figure S9. Comparison of the monthly averages of the IASI NH3 total column observations (Ω_{obs}) over the model horizontal land grid cells at $1.27° \times 2.5°$ resolution to the corresponding averages of the simulation of these observations with LMDZ-INCA model (Ω_{mod}) over different regions for the year 2019. Each panel shows the correlation coefficient (r), root mean square error (RMSE), and fractional bias (FB) between modeled (from both prior and IASI-constrained estimated NH3 emissions from inversions) and observed IASI NH3 columns. The left column in each panel displays results using prior CEDS NH3 emissions, while the right column displays results using the estimated NH3 emissions derived from our global inversions. The red dashed line represents the linear regression fit, and the black line denotes the 1:1 line.

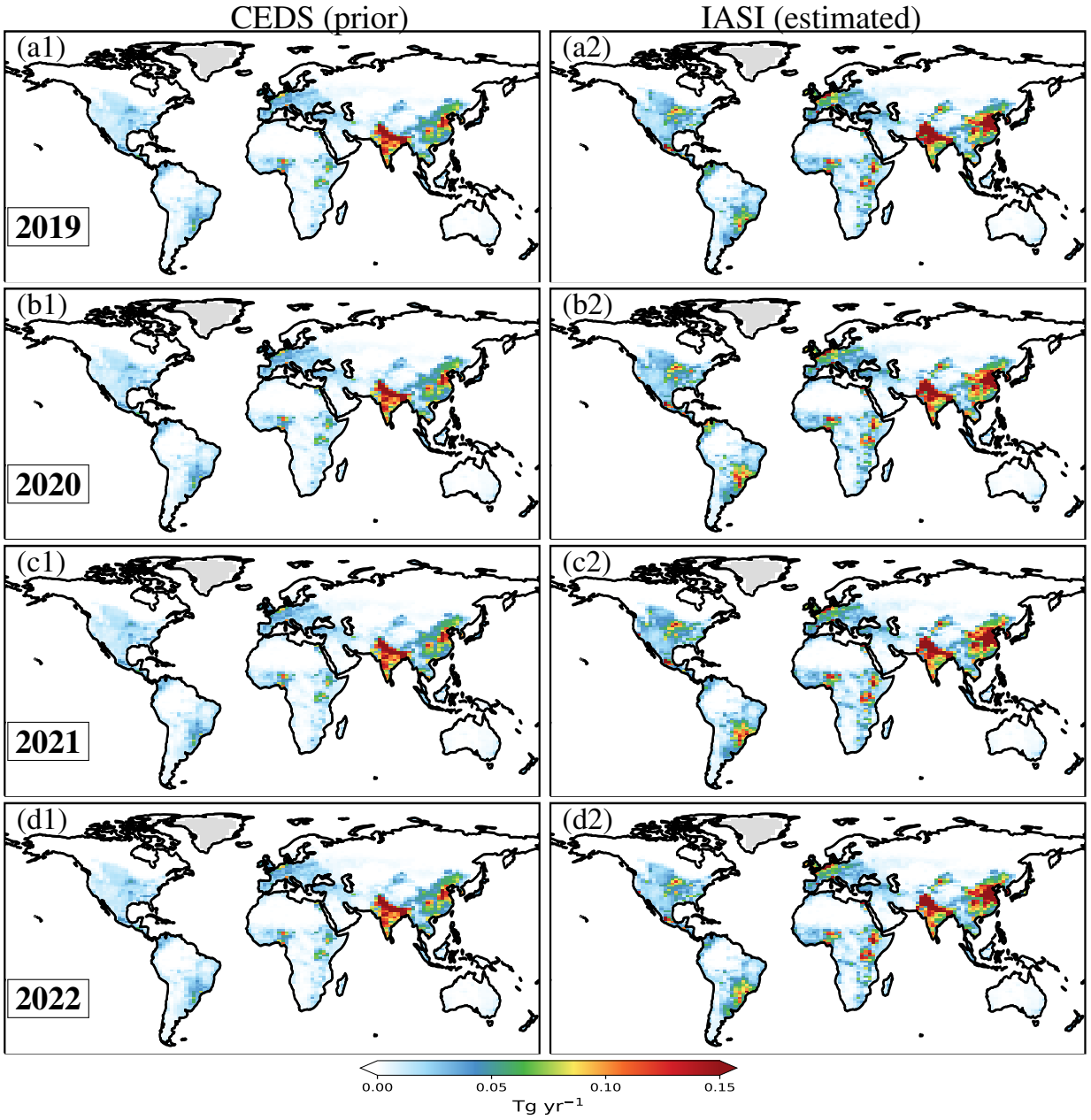

Figure S10. Spatial distribution of the total annual NH_3 emissions for a period of four years from 2019 to 2022, showing the bottom-up prior CEDS emissions (first column), and IASI-constrained emissions (second column).

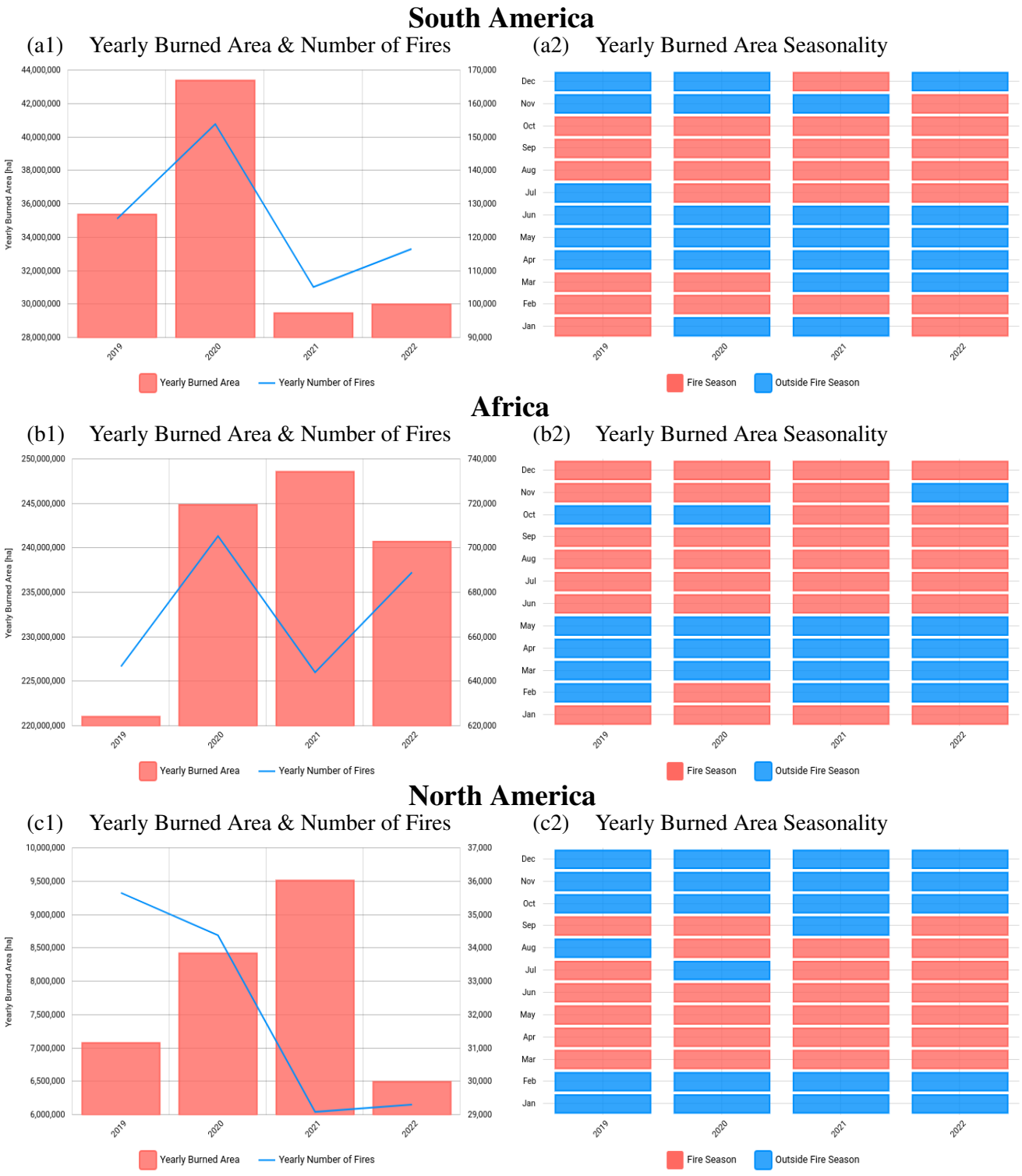

Figure S11. Yearly number of fires and burned area across the three regions (a) South America, (b) Africa, and (c) North America for the years from 2019 to 2022 (source: https://gwis.jrc.ec.europa.eu/, last access: 02-09-2024).

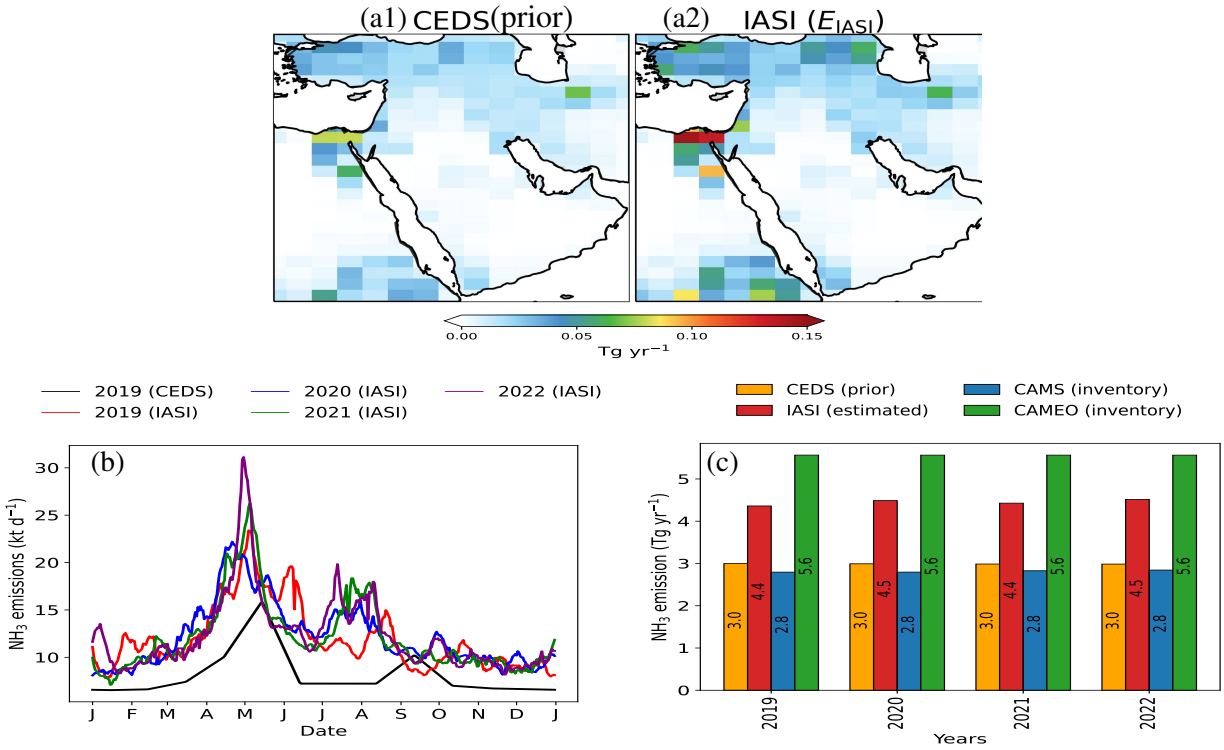

Figure S12. NH_3 Emissions over the Middle East region. First row shows the spatial distribution of the total annual emissions averaged over four-year period (2019-2022), showing (a1) the bottom-up prior CEDS emissions (first column), (a2) IASI-constrained emissions (E_{IASI}). Figure (b) shows the daily variation of the estimate NH_3 emissions for all four years and (c) shows the annual estimated, prior CEDS, and other bottom-up inventories emissions.